Field Study on Humidification Performance of a Desiccant Air-Conditioning System Combined with a Heat Pump

Authors:

Koichi Kawamoto, Wanghee Cho, Hitoshi Kohno, Makoto Koganei, Ryozo Ooka, Shinsuke Kato

Date Submitted: 2018-11-16

Keywords: heat pump, humidification, desiccant, dedicated outdoor air system (DOAS)

Abstract:

A desiccant air-conditioning system was developed as a latent-load-processing air conditioner in a dedicated outdoor air system during the summer. This study investigated the application of this air-conditioning system to humidification during the winter without using make-up water, thereby eliminating the cause of microbial contamination in air-conditioning systems. The experiments were conducted with a system used for summer applications to determine the feasibility of adsorbing vapor from outdoor air and supplying it to an indoor space. The humidification performance, energy efficiency, and operating conditions were examined. Although the conditions were subpar because the experiments were performed with an actual dedicated outdoor air system, the results showed that it is possible to supply air with a minimum humidity ratio of 5.8 g/kg dry air (DA) when the humidity ratio of outdoor air ranges from 1.8 to 2.3 g/kg DA. The minimum humidification performance required for a dedicated outdoor air system was achieved by increasing the airflow rate of the moisture-adsorption side to 2?3 times that of the humidification side. In addition, air leaking from the moisture-adsorption side to the humidification side, improving the mechanical structure, such as by the insulation of the moisture-adsorption side, and an efficient operating method were examined for humidification during the winter.

Record Type: Published Article

Submitted To: LAPSE (Living Archive for Process Systems Engineering)

Citation (overall record, always the latest version): LAPSE:2018.0842
Citation (this specific file, latest version): LAPSE:2018.0842-1
Citation (this specific file, this version): LAPSE:2018.0842-1v1

DOI of Published Version: https://doi.org/10.3390/en9020089

energies

MDPI

Article

Field Study on Humidification Performance of a Desiccant Air-Conditioning System Combined with a Heat Pump

Koichi Kawamoto [1], Wanghee Cho [2,*], Hitoshi Kohno [3], Makoto Koganei [4], Ryozo Ooka [5] and Shinsuke Kato [5]

1 Kawamoto Engineering, 3-1-11 Kami-Ikebukuro, Toshimaku, Tokyo 170-0012, Japan; kawamoto.koichi@silk.ocn.ne.jp
2 Department of Architecture, Faculty of Engineering, Kanagawa University, 3-27-1 Rokkakubashi, Kanagawa-ku, Yokohama 221-8686, Japan
3 Research and Development Center, Asahi Kogyosha Co., Ltd., 6-17-16 Higashi-Narashino, Narashino, Chiba 275-0001, Japan; hitoshi-kono@asahikogyosha.co.jp
4 Department of Architectural Design and Engineering, Graduate School of Science and Engineering, Yamaguchi University, 2-16-1 Tokiwadai, Ube, Yamaguchi 755-8611, Japan; mkoganei@yamaguchi-u.ac.jp
5 Institute of Industrial Science, The University of Tokyo, 4-6-1 Komaba, Meguro-ku, Tokyo 153-8505, Japan; ooka@iis.u-tokyo.ac.jp (R.O.); kato@iis.u-tokyo.ac.jp (S.K.)
* Correspondence: chowh@kanagawa-u.ac.jp; Tel.: +81-45-481-5661 (ext. 3477); Fax: +81-45-481-5360

Academic Editor: Vincent Lemort
Received: 2 October 2015; Accepted: 21 January 2016; Published: 30 January 2016

Abstract: A desiccant air-conditioning system was developed as a latent-load-processing air conditioner in a dedicated outdoor air system during the summer. This study investigated the application of this air-conditioning system to humidification during the winter without using make-up water, thereby eliminating the cause of microbial contamination in air-conditioning systems. The experiments were conducted with a system used for summer applications to determine the feasibility of adsorbing vapor from outdoor air and supplying it to an indoor space. The humidification performance, energy efficiency, and operating conditions were examined. Although the conditions were subpar because the experiments were performed with an actual dedicated outdoor air system, the results showed that it is possible to supply air with a minimum humidity ratio of 5.8 g/kg dry air (DA) when the humidity ratio of outdoor air ranges from 1.8 to 2.3 g/kg DA. The minimum humidification performance required for a dedicated outdoor air system was achieved by increasing the airflow rate of the moisture-adsorption side to 2–3 times that of the humidification side. In addition, air leaking from the moisture-adsorption side to the humidification side, improving the mechanical structure, such as by the insulation of the moisture-adsorption side, and an efficient operating method were examined for humidification during the winter.

Keywords: dedicated outdoor air system (DOAS); desiccant; humidification; heat pump

1. Introduction

Compared to conventional super-cooling dehumidification methods, a desiccant air-conditioning system can produce a dew-free environment inside both the air-conditioning system and indoor space during the summer. This has been reported as an effective method for reducing the degradation of the Indoor Air Quality (IAQ), which is caused by microbes, such as mold or bacteria [1–4]. In addition, many studies have been conducted on the application of desiccant air-conditioning systems as dedicated outdoor air systems (DOASs) during the summer [5–16].

A desiccant air-conditioning system can transfer vapor through the desiccant wheel, and thus, it is possible that such systems can be applied to humidification during the winter, as well as dehumidification during the summer. There have been reports of humidification-heating using a room air-conditioner in residential houses [17], using a liquid-type desiccant air-conditioning system [18–20], or recovering vapor from the indoor exhaust-airflow by coating the heat-pump coil with a desiccant [17]. Only few authors have investigated the wheel-type desiccant humidification method. De Antonellis *et al.* [21] proposed an air humidification system with desiccant wheel, which humidify an air stream by adsorbing water vapor from the outdoor air (OA), and examined the optimal system configuration and the effect of operation conditions on humidification by experimental tests and simulations. The higher ratio of the moisture-adsorption mass-flow rate to the humidification one, and the lower OA temperature could achieve a satisfactory humidification level in conditions of Southern Europe winter climate. La *et al.* [22] investigated the heating-humidification performance of a solar heating and humidification system with a one-rotor two-stage desiccant air-conditioning unit and estimated the optimal solar collector area. Solar heating with desiccant humidification could improve the indoor thermal comfort significantly, though return air (RA) was reused as humidification source. Wada *et al.* [23] developed a DOAS with desiccant wheel, which regenerated at a temperature of about 50 °C by using waste heat from water source heat pump, and showed that the humidification without using make-up water was possible if the humidity ratio of the OA was 3.5 g/kg dry air (DA) or above. However, this system basically required the RA for stable humidification. Fukudome [24] and Mathiprakasam [25] discussed the humidification-applicability of desiccant wheel primarily used for dehumidification. Most of the above studies were mainly conducted by measurements in laboratory facilities and/or numerical analysis. In addition, the research relevant to estimation of that humidification method using actual DOAS in actual outdoor condition has been rare, especially when the whole humidification source is secured from the OA without the RA.

Most of the commonly used humidification methods (evaporative, spray, and steam) require the drainage to be processed, which has a corresponding risk of microbes growing inside the air-conditioning unit under certain conditions. Evaporative humidification uses unheated water [26–29]. This may cause the growth of microbes in the humidifier during the summer or non-operating hours at night, as well as unpleasant odors. Spray humidification releases water directly into the air [30–33], and thus, any impurities and germs that are contained within the water are released into the air. Facilities where a degraded IAQ is not acceptable, such as hospitals, humidification methods that use unheated water should be avoided; *i.e.*, they use steam humidification [34–36]. With this method, even though the impurities in the water are not transported by the steam, there is still a risk of microbe growth in the drain pan and water tank. It also requires a greater level of maintenance because of the occasional buildup of limescale. When water is used as the source of humidity, a method of sterilizing the humidification filter and duct may be necessary, such as potassium chloride [37], microwaves or ozone [38–40], or ultraviolet germicidal irradiation (UVGI) [41,42].

The following benefits are expected from using a desiccant air-conditioning system that adsorbs the water vapor in the air and uses it for humidification, which is the focus of this study.

1. By adsorbing water vapor from the air and using it as the source of humidity instead of water, a water source and drain pan will not be necessary.
2. Peripheral equipment and piping work for heating and humidification, as well as the corresponding maintenance required to treat limescale, will not be necessary.
3. The risk of microbial growth inside the drain pan and water tank of the air-conditioning unit will be eliminated, and an improved IAQ is expected. A dew-free environment could be achieved both inside the air-conditioning unit and indoors throughout the year.
4. Under ideal conditions during the summer, where both the process and regeneration sides operate is isenthalpically, the regeneration energy is used to convert the latent-heat energy on the process side at the desiccant wheel to sensible-heat energy without reducing the enthalpy. To use high-temperature dehumidified air for cooling, its enthalpy must be reduced by a sensible-heat

exchange wheel and cooling coil. When the system is used for humidification during the winter, all of the regeneration energy put into the regeneration side, *i.e.*, the humidification side during the winter, is converted to enthalpy. Thus, a high-temperature air supply with increased humidity is obtained, thereby producing highly efficient humidification-heating compared to the process used for dehumidification during the summer.

With this method, insufficient humidification is a concern because it increases the humidity of the OA by pumping water vapor from the OA, which has low humidity ratio. To ensure a suitable humidification performance, a method was adopted to increase the airflow rate on the moisture-adsorption side (the process side during the summer) compared to that on the humidification side (the regeneration side during the summer). With this method, the following advantages and disadvantages are anticipated.

1. The amount of water vapor adsorbed by the wheel is increased by increasing the amount of water vapor in the OA supplied to the moisture-adsorption side.
2. Passing a large volume of low-temperature OA through the moisture-adsorption side quickly cools the wheel on the moisture-adsorption side, which increases the moisture-adsorption efficiency.
3. On the other hand, cooling the moisture-adsorption side slows the heating of the wheel on the humidification side, thereby reducing the desorption performance.

In this study, a desiccant air-conditioning system of a DOAS that was primarily used for dehumidification during the summer was used to perform humidification experiments in which water vapor was adsorbed from the OA and supplied to an indoor space for the purpose of humidification during the winter.

Despite the disadvantages of using an actual DOAS manufactured for summer dehumidification, the humidification performance, humidification efficiency, and efficient operating method of the desiccant air-conditioning system were investigated.

2. Outline of Experiment

2.1. Overview of the Experimental Setup

The authors developed the desiccant-based air-conditioning system in a previous study [4]. The proposed system was ameliorated by combining it with a heat pump for regeneration, and dehumidification experiments were performed. No other modifications were made to the desiccant air-conditioning system for evaluating its humidification performance during the winter. Figure 1 and Table 1 show the appearance and main elements of the experimental setup, respectively.

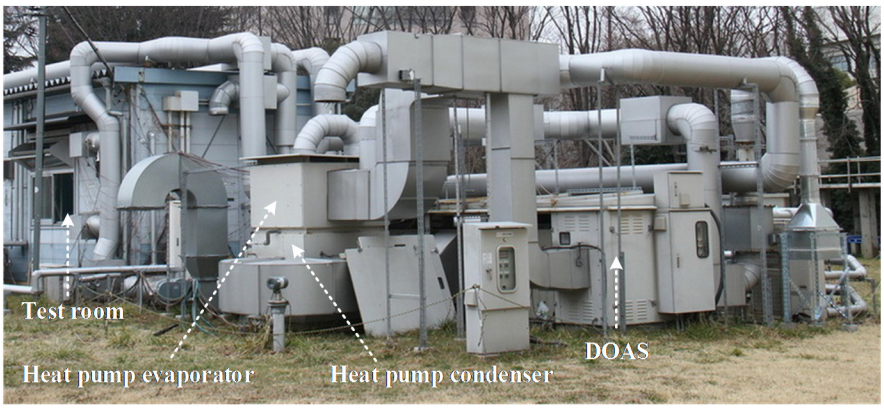

Figure 1. Appearance of the experimental setup.

Table 1. Specifications of the experimental setup.

Desiccant wheel		Silica gel; diameter = 800 mm; thickness = 200 mm; moisture-adsorption side = 0°–180°; humidification side = 180°–360°
Sensible-heat exchange wheel		Aluminum; diameter = 800 mm; thickness = 200 mm; moisture-adsorption side = 0°–180°; humidification side = 180°–360° nominal sensible-heat exchange efficiency = 75% (when the face air velocity on both sides is 3 m/s)
Regeneration heat pump	Evaporator	Cooling capacity = 7.2 kW (when the refrigerant boiling temperature is −5 °C and the air temperature to condenser is 32 °C); boiling was controlled by an electronic expansion valve
	Condenser	Heating capacity = 10.7 kW (when the refrigerant boiling temperature is −5 °C and the air temperature to condenser is 32 °C); finned-tube-type air-cooling; high-pressure control achieved with a microcomputer-controlled fan
	Compressor	Closed-loop; air-cooled refrigerant; condensing type; nominal output = 3.5 kW (when the refrigerant boiling temperature is −5 °C and the air temperature to condenser is 32 °C); vertical DC twin-rotary-type; refrigerant = R407C
Fans	Moisture-adsorption side (inlet)	Turbo fan; nominal power = 1.5 kW; fan is controlled by the frequency of the inverters
	Moisture-adsorption side (exhaustion)	Sirocco fan; nominal power = 3.7 kW; fan is controlled by the frequency of the inverters
	Humidification side (supply)	Turbo fan; nominal power = 0.75 kW; fan is controlled by the frequency of the inverters
Drive motor for wheels	Desiccant wheel	Geared motor; nominal power = 0.4 kW; motor is controlled by the frequency of the inverters
	Sensible-heat exchange wheel	Geared motor; nominal power = 0.4 kW; motor is controlled by the frequency of the inverters
Measuring instruments	Measuring points * 1, 3, 5, 7 and 8 for temperature and relative humidity	Temperature sensor = Pt100 RTD 1/3 class B IEC 751; polymer-type humidity sensor; temperature range = −40–100 °C; humidity (relative humidity) range = 0%–100%; accuracy of temperature measurements = ±0.2 °C; accuracy of humidity measurements = ±1% (0%–90%)
	Measuring points * 2, 4 and 6 for temperature	T-type thermocouple; measuring range = −40–350 °C; accuracy = ±1.5 °C
	Measuring points * 1, 5 and 7 for airflow rate	Measuring method = Multi-pitot tube traverse method according to Japanese Industrial Standards (JIS) B 8330; maximum range of airflow rate measurement = 6350 m^3/h; accuracy of airflow rate measurements = ±2%

* Note: See Figure 3b for the positions of the corresponding measuring points.

Figure 2 shows the dimensions of desiccant wheel and channel, measuring points of temperature at the outlet on the moisture-adsorption side of desiccant wheel. The desiccant wheel is made of honeycomb ceramic paper impregnated by silica gel. Figure 3 shows the operational flow of the experimental setup for summer dehumidification and winter humidification. The system used for this humidification study had been modified for several experiments during the summer. Therefore, the specifications of the desiccant wheel, capacity of the regeneration heat pump, insulation, pressure in the respective channels, *etc.*, were not optimized for winter humidification applications. In addition, the many bends, branches, and joints in the duct paths caused a large pressure drop because of these modifications. This resulted in large fan-shaft power consumption.

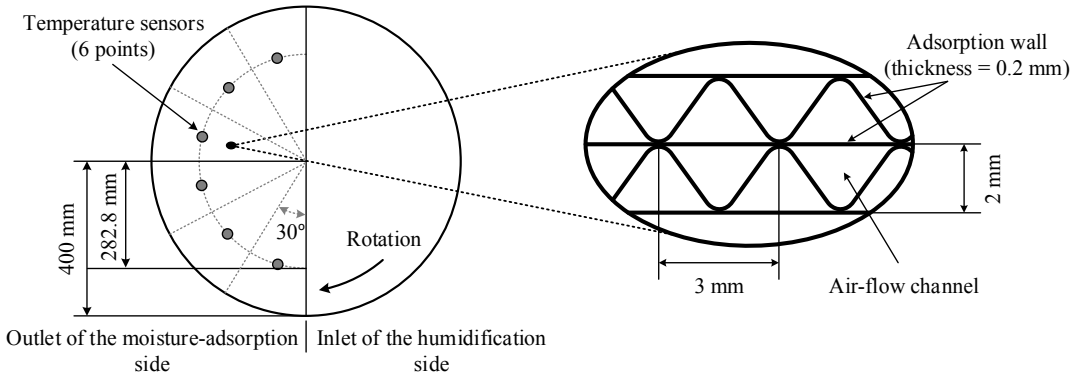

Figure 2. Dimensions of desiccant wheel and channel, and measuring points of temperature at the outlet on the moisture-adsorption side of desiccant wheel.

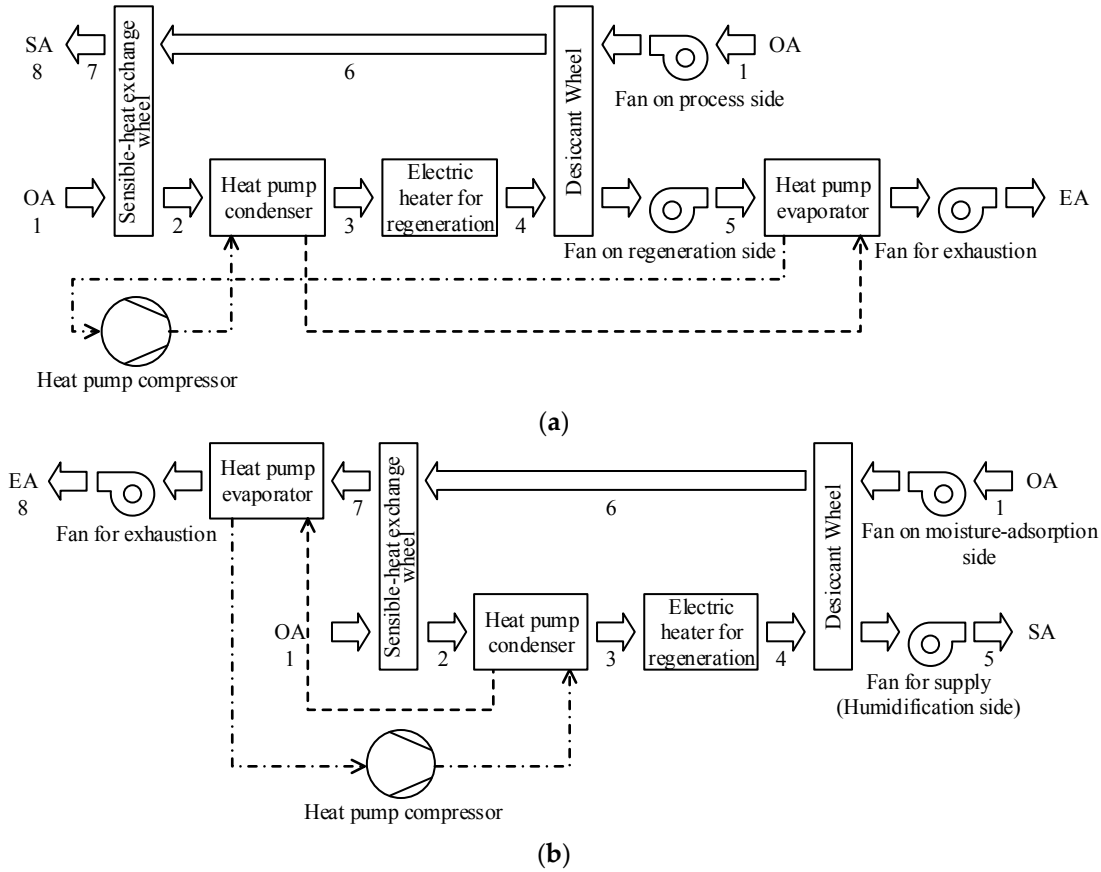

Figure 3. Operational flow of the experimental system for (**a**) summer dehumidification; and (**b**) winter humidification. SA = supply air; OA = outdoor air; EA = exhaust air.

2.1.1. System for Summer Operation

The system shown in Figure 3a is configured as a latent-load-processing DOAS. It is intended to improve the IAQ by creating a dew-free environment in the SA side. The energy efficiency of the DOAS is improved by combining it with a heat pump, which recovers the enthalpy from the high-temperature and high-humidity exhaust air (EA) of regeneration side. During summer operation, point 8 in Figure 3a indicates the SA on the process side (moisture-adsorption side or dehumidification side). Point 5 indicates the exhaust air on the regeneration side (humidification side during winter operation). The heat pump condenser and electric heater are positioned on the regeneration side to

regenerate the desiccant wheel. The heat pump evaporator cools the high-temperature, high-humidity EA of the regeneration side (point 5 in Figure 3a) and recovers the exhaust heat, thereby delivering high-efficiency regeneration of the desiccant wheel because of the high boiling temperature and dew-free environment of the SA side.

2.1.2. System for Winter Operation

In winter operation, point 8 in Figure 3b becomes the EA by switching the duct of the desiccant-based air-conditioning system in Figure 3a with the damper. Point 5 in Figure 3b is used as the SA on the humidification side (regeneration side during summer operation). The position of the heat pump evaporator is also switched with the damper to cool the EA (point 7 in Figure 3b) on the moisture-adsorption side. The characteristics of this operating method are as follows:

(1) The heat-pump condenser was placed upstream of the electric heater for regeneration. Therefore, when the heating of the desiccant wheel with the heat-pump condenser was insufficient, the electric heater was turned on.
(2) The sensible-heat exchange wheel was placed upstream of the heat pump condenser, which enabled the heating of the desiccant wheel, when necessary, by recovering the sensible energy from the high-temperature air caused by adsorption on the moisture-adsorption side.
(3) The air temperature at the condenser outlet was controlled at the upper limit, which was slightly below the high-pressure cut-out temperature (approximately 50 °C), by the DC inverter.
(4) The evaporator was positioned at the EA on the moisture-adsorption side. It pumped the heat from the high-temperature EA on the moisture-adsorption side to the humidification side and maintained the high-boiling temperature of the heat pump to enable high-efficiency operation. It also simultaneously cooled the low-humidity air after moisture-adsorption to minimize frost generation.
(5) The airflow rate was controllable at both the humidification and moisture-adsorption sides, and the evaporator was controlled with an electronic expansion valve to accommodate the changes in conditions.
(6) In the airflows of Figure 3b, the temperature of path point 2 → 3 → 4 → 5 after the sensible-heat exchange wheel on the humidification side was insulated, whereas path point 1 → 2 between the OA and after the sensible-heat wheel was not. Path point 7 → 8, downstream of the sensible-heat wheel on the moisture-adsorption side, was insulated, but path point 1 → 6 → 7 was not. This is because the experimental system was manufactured for summer dehumidification, where the air dehumidified by the desiccant wheel becomes warmer than the OA. Furthermore, cooling of the dehumidification path is required before the air is supplied. For heat dissipation to the OA, the insulation was not provided.
(7) The partial air of the moisture-adsorption side leaked to the humidification side via the sensible-heat exchange wheel. The detailed mechanisms of the air leakage are described in (2) of Section 3.1.

The humidification side that corresponds to the regeneration side during summer operation becomes the SA side during winter operation, and thus, the heat pump for heating the desiccant wheel, heating temperature, and heating energy were designated as the heat pump for regeneration, regeneration temperature, and regeneration energy, respectively. This was done to make them consistent with the components during summer operation.

2.2. Details of the Experiments

To improve the IAQ by achieving a dew-free environment, the humidification system was not operated in conjunction with an auxiliary humidification method. When considering its application as a DOAS, the system must steadily supply air with a minimum humidity ratio of 5.8 g/kg DA (humidity ratio at 20 °C and relative humidity 40% (the indoor set-point for humidification-heating)).

Table 2 shows the conditions tested in this study. The tests were conducted under two different OA conditions. The first experiment was conducted under a relatively high OA humidity (close to the amount of saturated water vapor) to verify the efficient operation method when the OA conditions are not inclement for humidification. The second experiment was performed with a low OA humidity ratio (close to the outdoor winter conditions used for designing an air-conditioning system in Japan, except Hokkaido area) to examine a method that achieves the aforementioned minimum humidification performance. It was assumed that drawing the EA (RA) from the indoor environment was not possible. Therefore, a method to pump in the required water vapor for humidification from the OA was adopted on the moisture-adsorption side (point 1 → 6 → 7 → 8 in Figure 3b).

To pump the moisture until the humidity ratio on the humidification side reached 5.8 g/kg DA at a low OA humidity ratio, the airflow rate on the humidification side was maintained at 500 m^3/h. The airflow rate on the moisture-adsorption side was controlled at either 500, 1000, or 1500 m^3/h. The regeneration temperature was set to 50, 60, or 70 °C.

Each airflow rate was set to and fixed by the frequency of the inverters for fans on the condition that the experimental system was running, *i.e.*, the heat pump for regeneration and the electric heater was operating, and the desiccant wheel was rotating. The average measured values of the airflow rate were stable but the actual value was varied within ±5% because of factors such as wind pressure.

Sensors on all measuring points except for point 4 and point 6 were set at the center of a sufficiently long and straight duct with an internal diameter of 300 mm. Nine thermocouples were set at measuring point 4, and the values were weight-averaged by the face air velocity at each point was adopted as the measured value, because this point was located in a narrow space between the heater and the desiccant wheel. The humidity on path point 2 → 3 → 4 of the humidification side was assumed to be the same value, and measured at measuring point 3. The measuring point at the outlet of the desiccant wheel on the humidification side had a large cross-sectional area; the humidity was measured at point 5 after well mixed by fan. At measuring point 6, the air temperature and humidity were not uniform with rotation angle because of the distribution of moisture-adsorption. Six thermocouples were set at measuring point 6 along with the rotating angle of the desiccant wheel (see Figure 2a), and the values were weight-averaged by the face air velocity. The humidity at the outlet of the desiccant wheel on the moisture-adsorption side was estimated at measuring point 7. Because the air leakage occurs from the moisture-adsorption side to the humidification side, the humidity at measuring points 6 and 7 was assumed as the same value.

The sensible-heat exchange wheel, which was used to increase the efficiency by recovering the adsorption heat from the air (point 6 in Figure 3b) on the moisture-adsorption side, was not rotated. This is because a large latent-heat carryover was observed in the preliminary experiments from the moisture-adsorption side (point 6 in Figure 3b) to the humidification side (point 2 in Figure 3b) when the sensible-heat exchange wheel was rotated. This significant leakage was caused by rotated air channels filled with moisture-adsorbed air of the sensible wheel from the moisture-adsorption side to the humidification side.

The airflow rate on the moisture-adsorption side was controlled by the only fan on the moisture-adsorption side, the fan for exhaustion on the moisture-adsorption side was not operated.

Table 2. Experimental conditions.

Experiment		**1st Experiment**				**2nd Experiment**	
Period of experiment		8–13 March 2012					
Location of experimental setup		1–8 Yayoicho, Inageku, Chiba 263–0022, Japan					
Outdoor conditions	Temperature (°C)	7–8				6–11	
	Humidity ratio (g/kg DA)	4.7–5.9				1.8–2.3	
	Atmospheric pressure (hPa)	1015					
Case		Case A1	Case A2	Case B1	Case B2	Case C1	Case C2
Airflow rate	Humidification side (supply) (m^3/h)	500					
	Moisture-adsorption side (inlet) (m^3/h)	500	1000	500	1000	1000	1500
Rotation speed of the desiccant wheel (rph)		5		10		5	
Regeneration temperature (°C)		50/60/70					
Heat pump compressor		Output changed to achieve the required regeneration temperature					
Rotation speed of the sensible-heat exchange wheel (rph)		0					

For each case, the temperature and humidity were measured and logged for a duration of 30 min with a measuring interval of 1 min after reaching the steady operating condition, which was obtained approximately 40 min following the running-in operation. These samples recorded values were averaged and used. Electric power for the heat pump was also logged in every one minute and averaged, but electric power for the heater was calculated by the airflow rate and the difference in temperature between point 3 and point 4 in Figure 3b. Electric power for each fan and drive motor of desiccant wheel was measured separately in operation.

For the first experiment, the measurements were taken under two different desiccant-wheel rotation speeds: 5 and 10 rph. However, because the faster rotation speed had a negligible effect on the performance of the desiccant wheel, the wheel speed was set to 5 rph for the second experiment.

3. Results and Discussion

To examine the accuracy of measurements [43,44], the results before averaging the experimental values in Case A1 under the condition that the regeneration temperature is 60 °C are plotted on time charts in Figure 4, as an example. The subscript-numbers of T and X in Figure 4a,b correspond to measurement points in Figure 3b. The values of ratio of temperature differences (σ_X) and ratio of humidity ratio differences (σ_T) were evaluated using Equations (1) and (2).

$$\sigma_T = \frac{T_5 - T_4}{T_6 - T_1} \tag{1}$$

$$\sigma_X = \frac{X_5 - X_4}{X_1 - X_7} \tag{2}$$

The values of X_1 and T_1 in Figure 4a,b show that the OA state was stable during measuring period. Because the OA of the inlet on humidification side was mixed with the leaked air from the moisture-adsorption side at measuring point 2 in Figure 3b, and the leaked air was dehumidified by desiccant wheel (see (2) of Section 3.1), the values of X_4 were lower than the ones of X_1. The values of T_5 and T_6 were relatively stable, although the values of T_4, regeneration temperature, were varying in a wave-like manner. This variation of the values of T_4 in Figure 4b was caused by the imperfect tuning of automatic controller for the regeneration temperature. The values of X_5 were not constant, which was in a slight contrast with the constant values of X_7. In Case A1, the airflow rate on humidification side and moisture-adsorption side were equal, 500 m^3/h. The values of σ_X and σ_T were equal to the ratio of mass rate, 1.11, ideally, considering that the density of moist air at measuring point 1 in Figure 3b was 1.25 and that at measuring point 5 in Figure 3b was 1.13. Figure 4c shows that σ_X was constant but slightly lower than 1.11. This difference indicates a small error of mass balance caused by the adjustment of airflow rate and measurement. In addition, because the measuring points for evaluation of σ_X and σ_T were not located just before and soon after the desiccant wheel, the sensible heat generated from fans, which located between desiccant wheel and measuring points, might influence on the states of air. However, the rise in temperature by fan was estimated at 1–2 °C, its influence is insignificant, considering the fluctuation band of OA temperature and maximum regeneration temperature of 70 °C. The waveform of the values of σ_T was caused by the wave-like variation of T_4. The values of σ_T were significantly larger than 1.11. The causes of this difference are examined in (6) of Section 3.1. In other cases, the dry-bulb temperature and humidity ratio of the OA listed in Table 2 were also relatively stable, considering the range of OA temperature, the ratio fluctuation band of OA temperature to maximum regeneration temperature of 70 °C.

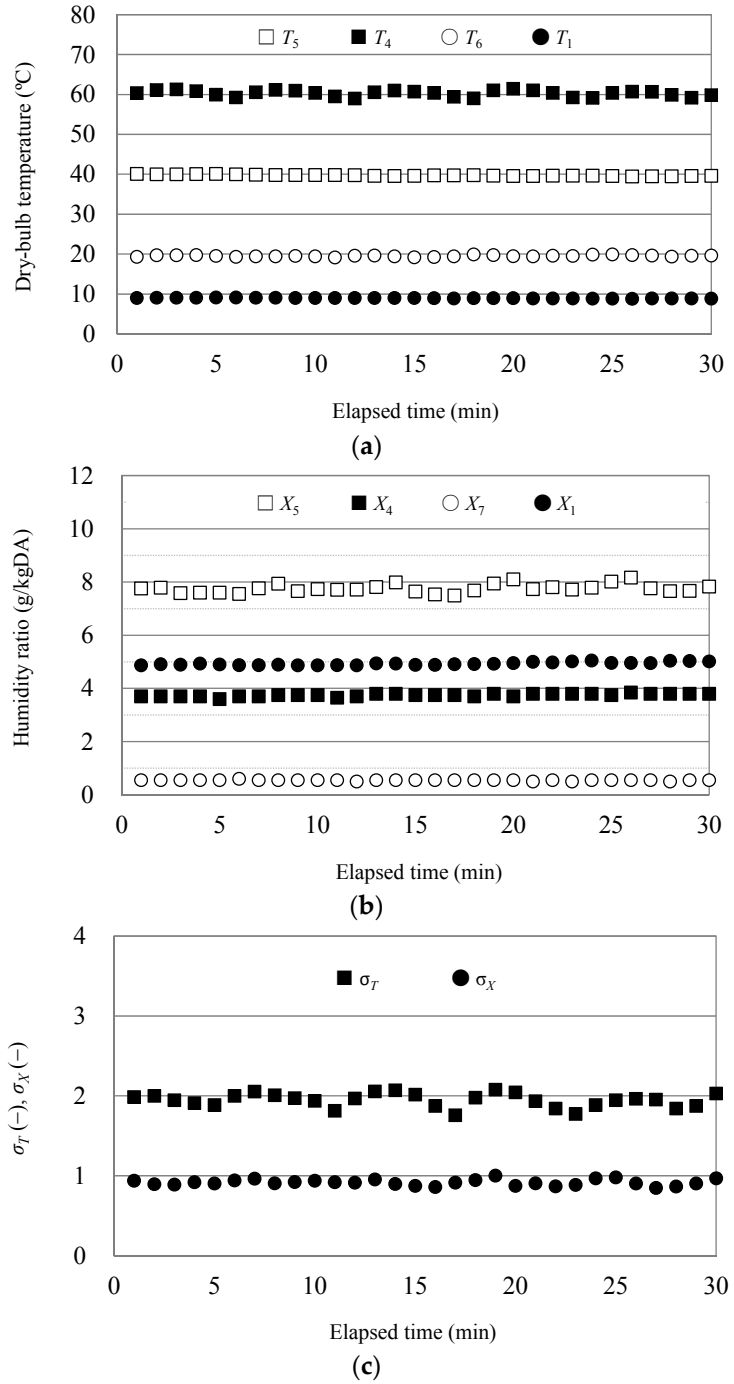

Figure 4. Experimental results of Case A1 at regeneration temperature of 60 °C on time charts for (**a**) inlet temperature and outlet temperature; (**b**) inlet humidity ratio and outlet humidity ratio; and (**c**) ratio of temperature differences and ratio of humidity ratio differences.

The results of the experiments performed under various conditions are plotted on psychrometric charts in Figure 5. The energy increments of the moisture-adsorption (point 1 → 6 in Figure 3b; see Section 3.1 for a detailed explanation) and humidification (point 4 → 5 in Figure 3b) sides of the desiccant wheel are shown alongside the latent and sensible heats in Figure 6. A positive value indicates an energy increment and a negative value indicates an energy decrement. All energy values shown in Figure 6 were calculated using Equations (3)–(8), by the mass rate depending on the density of moist air.

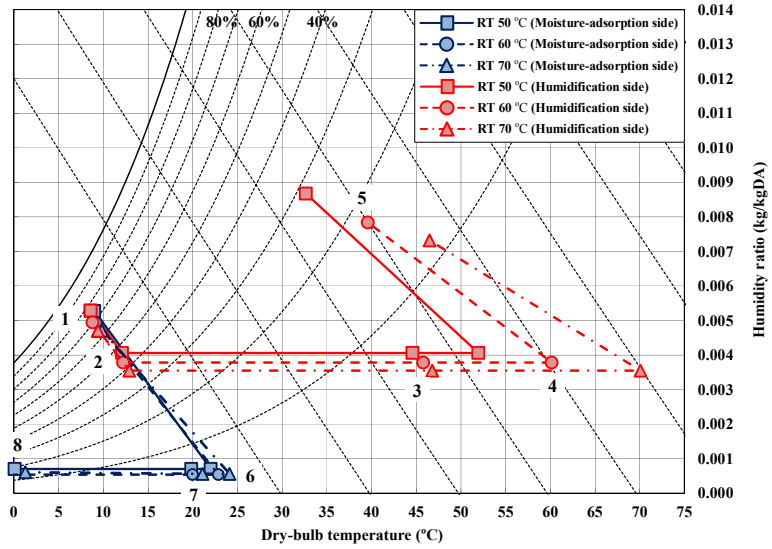

(**a**)

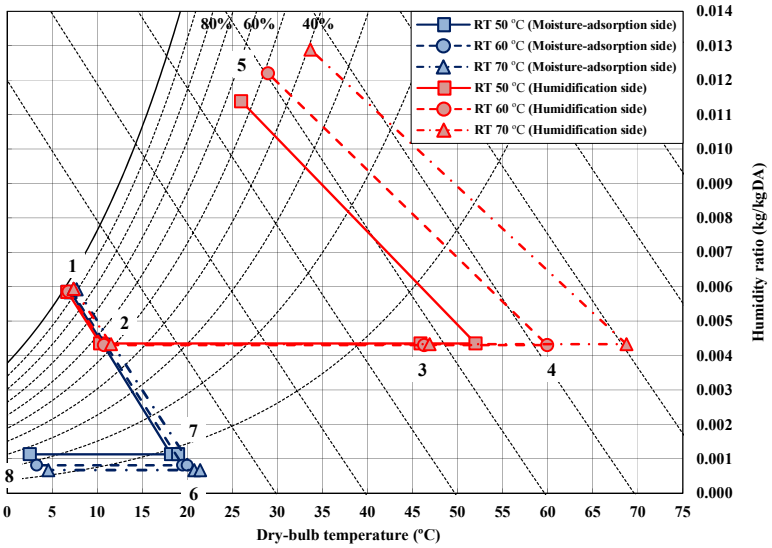

(**b**)

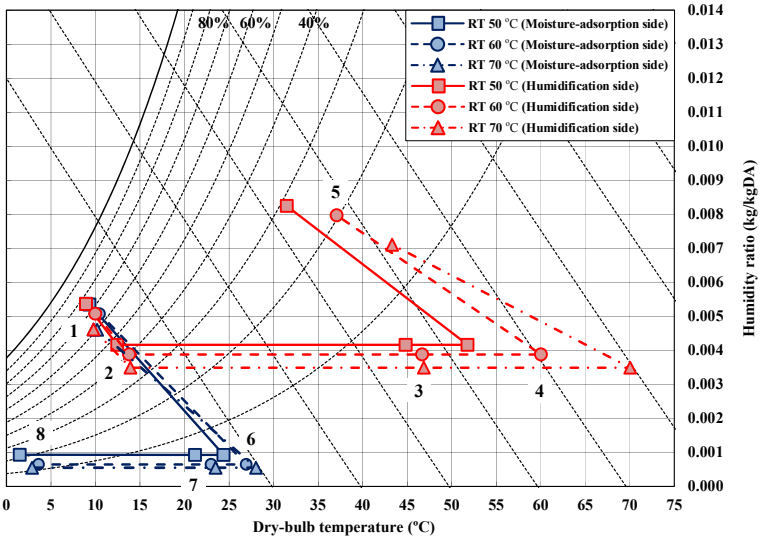

(**c**)

Figure 5. *Cont.*

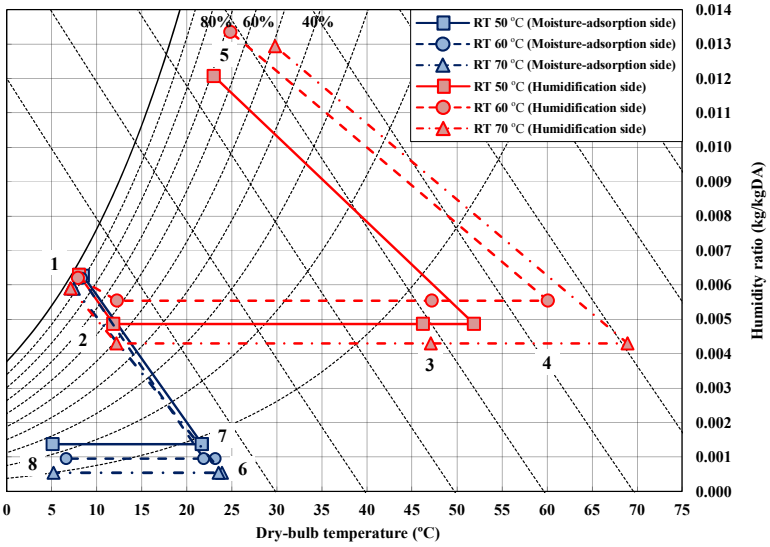

(**d**)

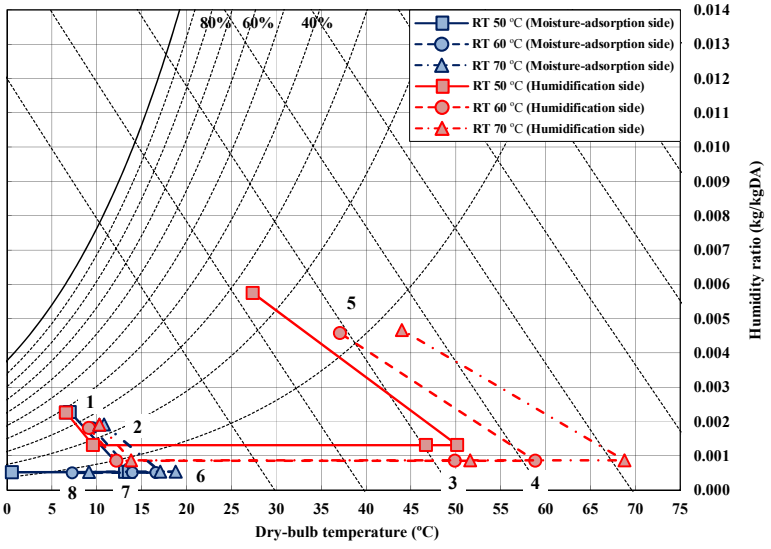

(**e**)

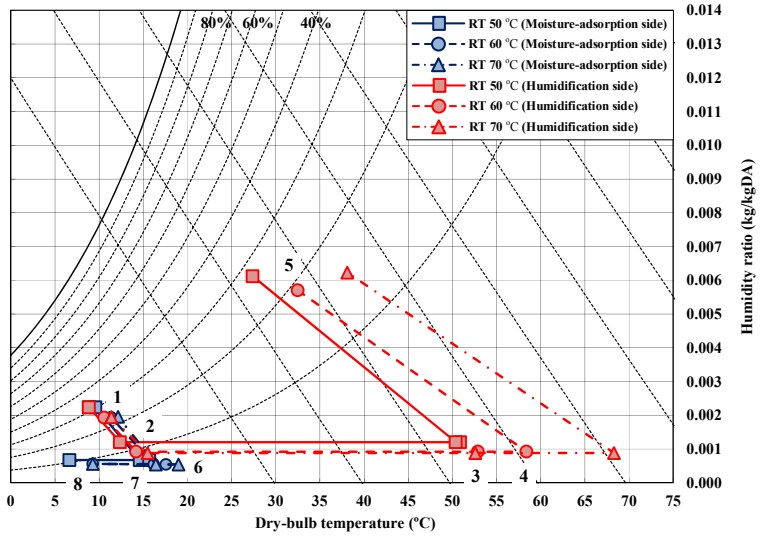

(**f**)

Figure 5. Plots of the experimental results on psychrometric charts for (**a**) Case A1; (**b**) Case A2; (**c**) Case B1; (**d**) Case B2; (**e**) Case C1; and (**f**) Case C2. RT = regeneration temperature.

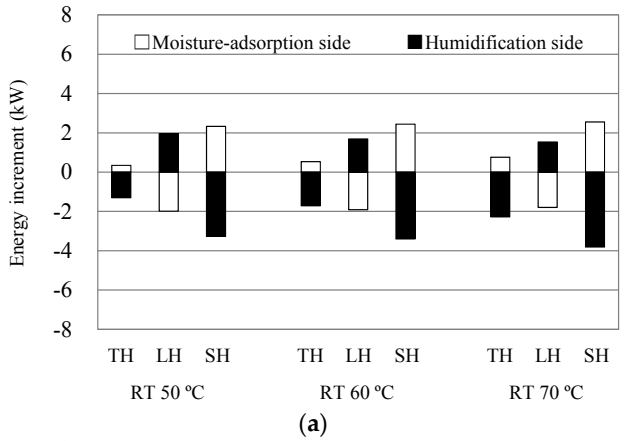

(**a**)

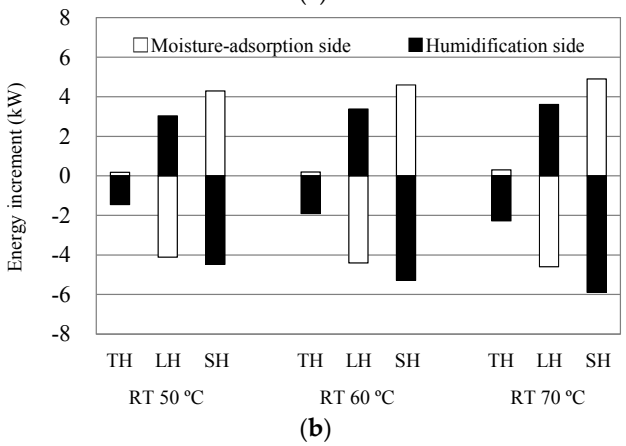

(**b**)

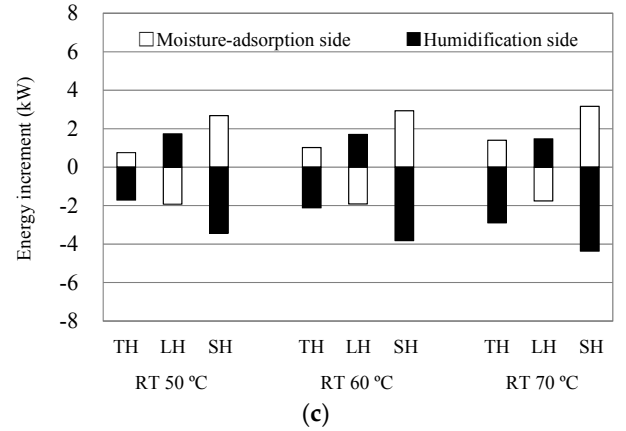

(**c**)

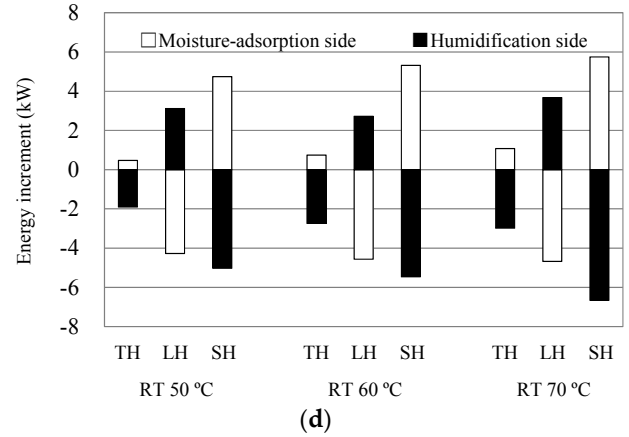

(**d**)

Figure 6. *Cont*.

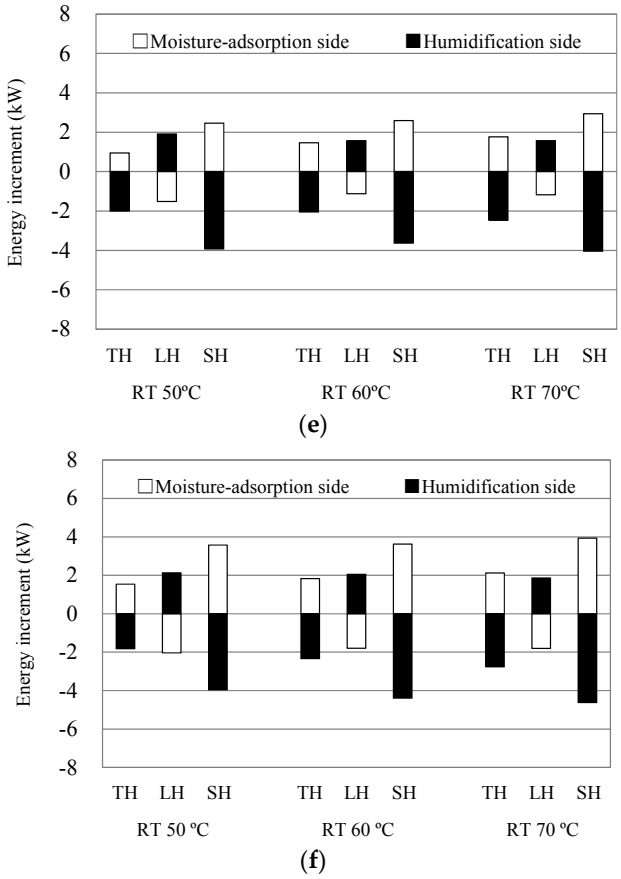

Figure 6. Energy increments for (**a**) Case A1; (**b**) Case A2; (**c**) Case B1; (**d**) Case B2; (**e**) Case C1; and (**f**) Case C2. TH = total heat; LH = latent heat; SH = sensible heat; RT = regeneration temperature.

$$EI_{TH\_M-A} = (H_6 - H_1) \times Q_1 \times \rho_1 \quad (3)$$

$$EI_{SH\_M-A} = (T_6 - T_1) \times cp_A \times Q_1 \times \rho_1 \quad (4)$$

$$EI_{LH\_M-A} = EI_{TH\_M-A} - EI_{SH\_M-A} \quad (5)$$

$$EI_{TH\_H} = (H_5 - H_4) \times Q_5 \times \rho_5 \quad (6)$$

$$EI_{SH\_H} = (T_5 - T_4) \times cp_A \times Q_5 \times \rho_5 \quad (7)$$

$$EI_{LH\_H} = EI_{TH\_H} - EI_{SH\_H} \quad (8)$$

Figures 5a,b and 6a,b show the results of the first experiment when the desiccant wheel was rotated at 5 rph, while Figures 5c,d and 6c,d show the experimental results when the desiccant wheel was rotated at 10 rph. Finally, Figure 5e,f, and Figure 6e,f show the results of the second experiment, where the desiccant wheel was rotated at 5 rph. The numbers 1–8 in Figure 5 correspond to measurement points 1–8 in Figure 3b.

Table 3 shows the electric energy consumption of the regeneration heat pump (E_{R_HP}), the electric heater (E_{R_EH}), fans (E_F) and the drive motor of desiccant wheel (E_W). These values were used in calculation of the coefficient of performances (*COP*s). Figure 7 shows the heating efficiency of the heat pump for regeneration (COP_{R_HP}), humidification-heating efficiency of the heat-source side (COP_{HH}), and the humidification-heating efficiency of whole system (COP_{SYS}) under each set of experimental conditions; the aforementioned *COP* values were evaluated using Equations (9)–(11), respectively. The COP_{HH} and COP_{SYS} values were calculated from the difference in enthalpy of the inlet and outlet on the humidification side.

Table 3. Electric energy consumption.

Title	Case A1			Case A2			Case B1			Case B2			Case C1			Case C2		
RT * (°C)	50	60	70	50	60	70	50	60	70	50	60	70	50	60	70	50	60	70
E_{R_HP} (kW)	3.381	3.490	3.367	3.466	3.143	3.138	3.467	3.361	3.241	3.237	3.098	3.009	3.180	3.215	2.875	3.038	3.072	2.945
E_{R_EH} (kW)	1.243	2.372	3.764	1.051	2.328	3.668	1.178	2.222	3.784	0.986	2.223	3.714	0.598	1.495	2.806	0.000	0.933	2.609
E_F (kW)	0.797			0.910			0.797			0.910			0.910			0.945		
E_W (kW)	0.014						0.016						0.014					

* Note: RT = regeneration temperature.

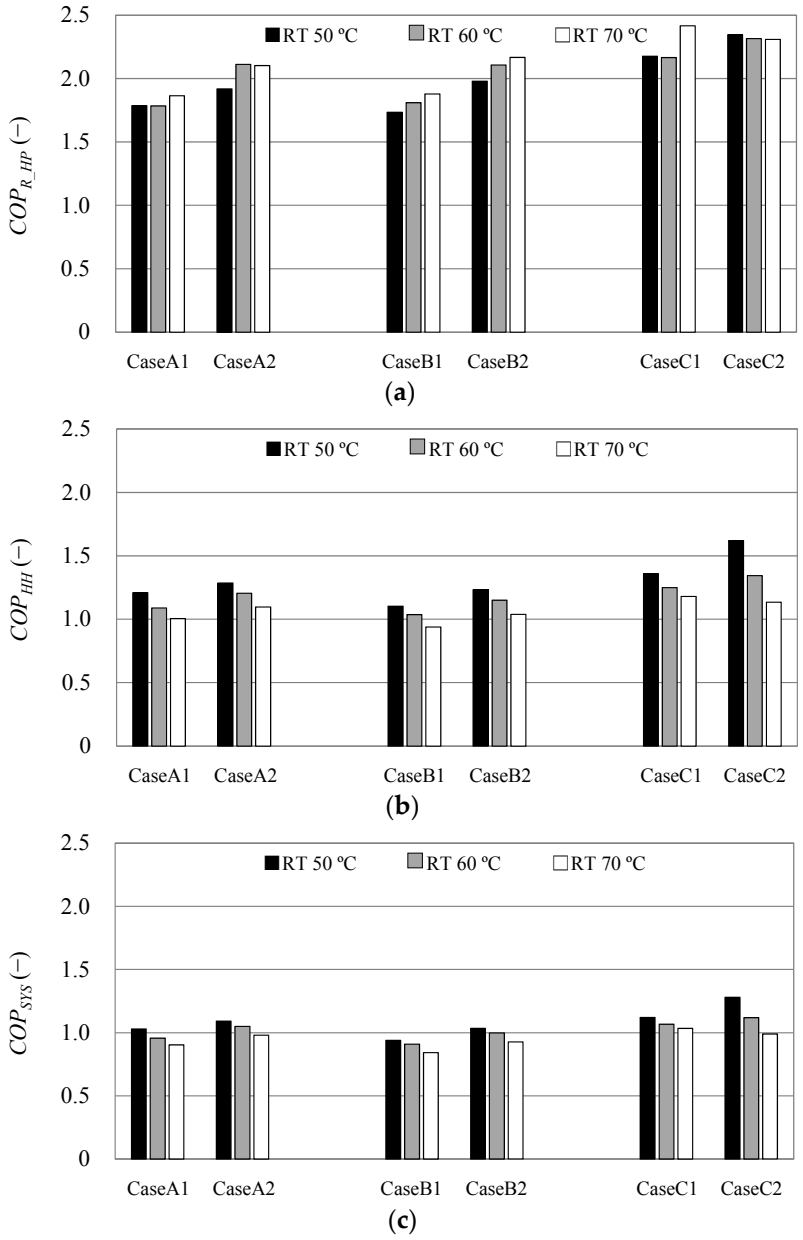

Figure 7. (**a**) Heating efficiency of the heat pump for regeneration (COP_{R_HP}), (**b**) Humidification-heating efficiency of the heat-source side (COP_{HH}), (**c**) Humidification-heating efficiency of the whole system (COP_{SYS}). RT = regeneration temperature.

$$COP_{R\_HP} = \frac{(H_3 - H_2) \times Q_5 \times \rho_5}{E_{R\_HP}} \quad (9)$$

$$COP_{HH} = \frac{(H_5 - H_1) \times Q_5 \times \rho_5}{E_{R\_HP} + E_{R\_EH}} \quad (10)$$

$$COP_{SYS} = \frac{(H_5 - H_1) \times Q_5 \times \rho_5}{E_{R\_HP} + E_{R\_EH} + E_F + E_W} \quad (11)$$

3.1. Humidification Performance

The following conclusions were drawn from the humidity ratios of the air and energy increments before and after the desiccant wheel in Figures 5 and 6 respectively.

(1) Figure 5e,f indicate that the minimum humidity ratio of 5.8 g/kg DA is achieved at the outlet on the humidification side (SA or point 5 in Figure 3b) under certain operating conditions, even when the humidity ratio of the OA was approximately 2 g/kg DA in the second experiment. This satisfies the minimum humidification performance requirements of a DOAS in most areas of Japan. The required humidification performance is achievable by selecting the appropriate parameters, such as increasing the airflow rate on the moisture-adsorption side or increasing the regeneration temperature.

(2) In all of the cases shown in Figure 5, a reduction of the humidity ratio occurs for path point 1 → 2 of the humidification side in Figure 3b. This is caused by the air leaking from the moisture-adsorption side to the humidification side via the sensible-heat exchange wheel. In a typical desiccant air-conditioning system for summer dehumidification, the degradation of the dehumidification performance is due to the inflow of high-humidity air from the regeneration side (humidification side during winter operation) to the process side (moisture-adsorption side during winter operation). To prevent this dehumidification performance degradation, a fan is positioned on the process side to push the humid air away, and another fan is positioned on the regeneration side to pull the air out. This arrangement maintains a positive pressure on the dehumidification side with respect to the regeneration side. In addition, to prevent the transportation of air from the regeneration side to the process side via the rotation of the sensible-heat exchange wheel, a channel is created in a portion of the wheel that allows the air on the process side to pass through. This intentionally permits some of the air on the process side to flow to the regeneration side. In this study, this setup also caused the air to leak from the moisture-adsorption side to the humidification side, reducing the efficiency of the DOAS for humidification applications.

(3) Once the operation of the desiccant air-conditioning system becomes stable, the size of the latent-heat energy decrement on the moisture-adsorption side (point 1 → 6 in Figure 3b) becomes equal to the latent-heat energy increment on the humidification side (point 4 → 5 in Figure 3b). Each case in Figure 6 also shows that the increments and decrements in the latent-heat energy at the desiccant wheel are approximately equivalent.

(4) Normally, both the level of moisture-adsorption and humidification of the desiccant wheel increase as the regeneration temperature increases. However, the levels of moisture-adsorption (size of the latent-heat energy decrement on the moisture-adsorption side) and humidification (size of the latent-heat energy increment on the humidification side) are almost constant in Figure 6a,c,e,f, regardless of the regeneration temperature. The minimum values for the humidity ratio after moisture-adsorption (point 6 in Figure 3b) in all of the cases shown in Figure 5 range from 0.5 to 0.7 g/kg DA. Therefore, it can be concluded that the lowest possible humidity ratio after moisture-adsorption (point 6 in Figure 3b) in this experimental setup is 0.5 g/kg DA, and neither the level of dehumidification nor that of humidification can increase once this limit is reached. Most of the water vapor in the OA is adsorbed at this lower limit by the wheel and

released to the humidification side, regardless of the regeneration temperature. On the other hand, in Figure 6b,d, both the level of moisture-adsorption and humidification increase slightly as the regeneration temperature increases. This is probably because the humidity ratio of the OA (point 1 in both Figure 5b,d) was high, and thus, the potential for moisture-adsorption was higher than in the other cases.

(5) Comparison of Figure 6a–f shows that the level of humidification increases as the airflow rate on the moisture-adsorption side is increased with respect to the flow on the humidification side.

(6) In all of the cases shown in Figure 6, the absolute value of the sensible-heat energy increment on the moisture-adsorption side, which should be nearly identical for all cases, is smaller than the absolute value of the sensible-heat energy decrement on the humidification side. A slight difference between the increment and decrement of the latent-heat energy is also observed, but it is small compared to that of the sensible-heat energy. Therefore, this difference between the increment and decrement of the sensible-heat energy is attributed to the difference between the gradients of the moisture-adsorption side (point 1 → 6 in Figure 3b) and humidification side (point 4 → 5 in Figure 3b) on the psychrometric charts (Figure 5). It is also attributed to the difference between the increment of the total heat energy on the moisture-adsorption side (point 1 → 6 in Figure 3b) and its decrement on the humidification side (point 4 → 5 in Figure 3b), as shown in Figure 6. These phenomena are assigned to the loss of sensible-heat energy (heat that is released from the air-conditioning system to the low-temperature OA during the winter) on the moisture-adsorption side. This loss of sensible-heat energy is caused by path point 1 → 6 → 7 on the moisture-adsorption side because it is not insulated, while path point 2 → 3 → 4 → 5 on the humidification side is insulated (see Figure 3b). Thus, if path point 1 → 6 → 7 on the moisture-adsorption side in Figure 3b were insulated, it can be expected that the air temperature of point 8 and the boiling temperature of the heat pump increase, which in turn improves the efficiency of the heat pump. In addition, no frost was observed on the evaporator side during any of the experiments.

3.2. Efficiency of the System

The following conclusions were drawn from the values calculated for COP_{R_HP}, COP_{HH}, and COP_{SYS} under the various experimental conditions, as shown in Figure 7.

(1) The shape of the ducts and fans in this experimental setup were not optimized for winter operation, and therefore, the COP_{HH} values were evaluated by only considering the heat pump for regeneration and the electric heater. In addition, the power consumption of the fan and rotating power of the wheel were excluded. Figure 7b indicates that the COP_{HH} values range from 0.8 to 1.59, which are very low efficiency values for a heat-pump-assisted system. The possible causes for this are as follows:

   (a) The lines representing the moisture-adsorption side of the desiccant wheel (point 4 → 5 in Figure 3b) are more inclined towards the left-hand side than the isenthalpic line in the psychrometric charts (Figure 4), indicating a substantial enthalpy loss, which is primarily caused by a transfer of sensible-heat energy from the humidification side to the moisture-adsorption side. The enthalpy transferred from the humidification side (the regeneration side during summer operation) to the moisture-adsorption side (the process side during summer operation) occurs because of the rotation of the desiccant wheel, regardless of the season. Compared to the summer operation for dehumidification, the air temperature in the moisture-adsorption side and the temperature of the OA are relatively low during winter operation, and thus, the heat released from the humidification side to the moisture-adsorption side and OA is larger than that during summer operation. Figure 6 shows that the total heat loss on the humidification side increases as the regeneration temperature increases while all of the other conditions remain the same. This confirms that

the temperature differential between the humidification and moisture-adsorption sides is the major cause of the total heat loss. Comparison of Figure 6a,b, Figure 6c,d, Figure 6e,f show that there are no significant difference in the total heat loss on the humidification side, even when the airflow rate on the moisture-adsorption side is increased. Regarding the effect of the rotating speed of the desiccant wheel, there is no substantial difference in the total heat-energy loss on the humidification side, as shown by comparing Figure 6a,c, Figure 6b,d. However, the total heat-energy losses are slightly greater at 10 rph (Cases B1 and B2) than at 5 rph (Cases A1 and A2). It is believed that the speed of the desiccant wheel affects the level of sensible-heat transportation.

(b) The condensation temperature of the heat pump for regeneration is high at approximately 50 °C. The boiling temperature of the heat pump, which was estimated from the temperature measured at point 8 in Figure 3b, is low at 0 °C and below. This results in the low efficiency of the heat pump.

(c) The heat pump was operating under a partial load.

(2) For each case, as the regeneration temperature decreased, the operating rate of the low-efficiency electric heater was also decreased. Conversely, both the $COP_{HH}$and COP_{SYS} values tend to increase.

(3) When the other conditions are the same, both the COP_{HH} and COP_{SYS} values increase faster as the airflow rate on the moisture-adsorption side increases with respect to the flow on the humidification side. It is concluded that the main reason for the improved efficiency is that the quantity of heat transferred from the heat pump condenser to the humidification side is approximately the same. This also causes the quantity of heat to cool the moisture-adsorption side to be approximately equal. The increasing temperature of point 8 in Figure 3 is due to the increased airflow rate on the moisture-adsorption side increasing the boiling temperature of the heat pump. The COP_{R_HP} values are also higher when the airflow rate of the moisture-adsorption side is set at 1000 m^3/h instead of 500 m^3/h.

(4) In Figure 7, a comparison of Cases A1 and B1, and Cases A2 and B2 shows that the *COP* values are slightly higher when the rotation speed of the desiccant wheel is 5 rph (Cases A1 and A2) instead of 10 rph (Cases B1 and B2). The differences between the total heat-energy losses on the humidification side, as previously discussed, are believed to affect these results. No overall tendency can be inferred from the results in Figure 7b for the effect of the rotation speed of the desiccant wheel on the COP_{R_HP} value of the heat pump. The efficiency can be improved slightly by applying an optimal rotation speed to the desiccant wheel.

4. Conclusions

This study experimentally evaluated the humidification performance of a desiccant air-conditioning system that was combined with a heat pump. To improve the regeneration efficiency of the heat pump, the heat pump evaporator was positioned at the EA on the moisture-adsorption side.

The results of this study, which was performed with an actual DOAS under two different OA conditions, allowed the following conclusions to be drawn.

(1) Even under OA conditions that were the equivalent of the outdoor winter conditions for designing an air-conditioning system, a humidity ratio of 5.8 g/kg DA or more was achieved for the SA by selecting the appropriate parameters, such as increasing the airflow rate on the moisture-adsorption side or increasing the regeneration temperature. In addition, it was confirmed that the system satisfied the minimum level of humidification performance required for a DOAS in Japan.

(2) The configuration of the air-conditioning system was optimized for dehumidification, and therefore, the air leaking from the moisture-adsorption side to the humidification side substantially reduced the humidification performance. To use the desiccant air-conditioning system for winter humidification, its structure must be improved to minimize such leaks.

(3) It is desirable to keep the sensible-heat exchange wheel stationary because the negative effects, which are due to the transportation of latent heat from the moisture-adsorption side to the humidification side by rotation, are greater than the adsorption heat recovered by the rotation of the sensible-heat exchange wheel.

(4) In the case of a desiccant air-conditioning system that is combined with a heat pump for winter humidification, the moisture-adsorption side should be insulated to improve the efficiency of the heat pump for humidification-heating.

(5) The COP_{SYS} and COP_{R_HP} values in an actual controlled operation will be higher than the ones shown in Figure 7 in most cases. The dew-points of SA were higher than the required one. To obtain the required dew point, an automatic controller would calculate and set a lower regeneration temperature than that in this experiment. Lower controlled regeneration temperature by automatic controller leads higher COP_{SYS} and COP_{R_HP} values by reducing the operation of the low efficient electric heater or the lower condensation temperature of the heat pump.

(6) Air leakage on the humidification side (point 1 → 2 in Figure 3b) causes a larger amount of humidification at the set dew-point of SA in an actual controlled operation. A smaller amount of humidification due to no leakage requires a lower regeneration temperature lower. This also leads higher COP_{SYS} and COP_{R_HP} values by reducing the operation of the low efficient electric heater or the lower condensation temperature of the heat pump. Improvement rate of the COP_{SYS} and COP_{R_HP} values depends on outdoor air conditions.

(7) The lowest possible humidity ratio after moisture-adsorption with this system was 0.5 g/kg DA. Neither the level of moisture-adsorption nor that of humidification was improved by increasing the regeneration temperature once this limit was reached.

(8) By increasing the airflow rate of the moisture-adsorption side with respect to the rate on the humidification side, the level of humidification increased approximately in proportion to the increase in the airflow rate on the moisture-adsorption side.

(9) The COP_{R_HP}, COP_{HH}, and COP_{SYS} values were also improved when the airflow rate on the moisture-adsorption side was increased with respect to the flow on the humidification side.

From the above results, it can be concluded that it is advantageous to augment the airflow rate on the moisture-adsorption side with respect to the flow rate on the humidification side for the highly efficient operation of a desiccant air-conditioning system, which is combined with a heat pump, as a humidifying device. The reasons for this are as follows:

(a) The boiling temperature of the evaporator of the heat pump used for humidification-heating at the downstream of the moisture-adsorption side rises, thereby increasing the efficiency of the heat pump.

(b) In addition, increasing the boiling temperature of the evaporator can minimize the possibility of frost.

(c) A high humidity ratio in the SA can be achieved, even when the humidity ratio of the OA is low. This makes it possible to restrict the regeneration temperature to low values to obtain the same humidity ratio at the outlet, which also reduces the input energy.

(d) Controlling the level of humidification (dew-point of the SA) by varying the regeneration temperature can reduce the operating rate of the low-efficiency electric heater when the heat-pump capacity is insufficient. Even when its capacity is sufficient and the electric heater is not operating, reducing the compressor speed increases the boiling temperature when under a constant condensation temperature. This is expected to increase the scale of the efficiency improvements. When the humidity ratio of the OA is low, the moisture is only adsorbed to the adsorption limit of the desiccant wheel, even if the regeneration temperature is increased. By setting the humidity ratio after moisture-adsorption to the adsorption limit (0.5 g/kg DA in the case of this study) to control the lower limit of the regeneration temperature, it is possible that unnecessary energy inputs can be avoided.

As described above, stable humidification-heating is believed to be possible when the maximum COP_{HH} value of this study (1.62) is obtained. The COP_{HH} value of 1.62 is inferior in terms of primary energy consumption to that of the conventional humidification-heating method of using a boiler. Therefore, to improve the humidification-heating performance, it is believed that ameliorating the mechanisms of the air-conditioning system is required, such as improving the efficiency of the heat pump for regeneration, enhancing the insulation of the equipment, and minimizing the air leakage from the moisture-adsorption side to the humidification side.

As future work, investigation into the optimization of the desiccant system and the improvement of dehumidification/humidification performance by numerical analysis [11,18] will be accomplished.

Author Contributions: Koichi Kawamoto performed the main experiments, wrote the paper, and analyzed the experimental results; Wanghee Cho provided guidance and supervision; Hitoshi Kohno and Makoto Koganei conceived and designed the experiments, and executed the experiments; and Ryozo Ooka and Shinsuke Kato reviewed the paper. All authors have read and approved the final manuscript.

Conflicts of Interest: The authors declare no conflict of interest.

Nomenclature

σ_T	Ratio of temperature differences, dimensionless value
T_N	Dry-bulb temperature at the measuring point N in Figure 3b, °C
σ_X	Ratio of humidity ratio differences, dimensionless value
X_N	Humidity ratio at the measuring point N in Figure 3b, kg/kg DA
$EI_{TH\_M\text{-}A}$	Total heat increment of desiccant wheel on the moisture-adsorption side, kW
H_N	Enthalpy at the measuring point N in Figure 3b, kJ/kg
Q_N	Airflow rate at the measuring point N in Figure 3b, m^3/s
ρ_N	Density of moist air at the measuring point N in Figure 3b, kg/m^3
$EI_{SH\_M\text{-}A}$	Sensible heat increment of desiccant wheel on the moisture-adsorption side, kW
cp_A	Specific heat of air, kJ/(kg· K)
$EI_{LH\_M\text{-}A}$	Latent heat increment of desiccant wheel on the moisture-adsorption side, kW
EI_{TH_H}	Total heat increment of desiccant wheel on the humidification side, kW
EI_{SH_H}	Sensible heat increment of desiccant wheel on the humidification side, kW
EI_{LH_H}	Latent heat increment of desiccant wheel on the humidification side, kW
COP_{R_HP}	Heating efficiency of the heat pump for regeneration, dimensionless value
COP_{HH}	Humidification-heating efficiency on the heat-source side, dimensionless value
E_{R_HP}	Electric energy consumption of the heat pump for regeneration, kW
E_{R_EH}	Electric energy consumption of electric heater, kW
COP_{SYS}	Humidification-heating efficiency of the whole system, dimensionless value
E_F	Electric energy consumption of the fans (fan on the moisture-adsorption side and supply fans in Figure 3b), kW
E_W	Electric energy consumption of the rotating motor for the desiccant wheel, kW

References

1. Burge, S.; Hedge, A.; Wilson, S.; Bass, J.H.; Robertson, A. Sick building syndrome: A study of 4373 office workers. *Ann. Occup. Hyg.* **1987**, *31*, 493–504. [CrossRef] [PubMed]
2. Bluyssen, P.M.; Cox, C.; Seppänen, O.; de Oliveira Fernandes, E.; Clausen, G.; Müller, B.; Roulet, C.A. Why, when and how do HVAC-systems pollute the indoor environment and what to do about it? The European AIRLESS project. *Build. Environ.* **2003**, *38*, 209–225. [CrossRef]
3. Wolfe, E.I. Desiccants' Experimental Performance Characteristics and Effectiveness as an Air Conditioning System. Master's Thesis, Lehigh University, Bethlehem, PA, USA, 1 December 1993.

4. Tsay, Y.S.; Kato, S.; Ooka, R.; Koganei, M.; Nishida, K.; Kawamoto, K. Study on noncondensing air-conditioning system performance when combining a desiccant cooling system with a CO_2 heat pump. *Hvac R Res.* **2006**, *12*, 917–933. [CrossRef]
5. Liu, X.; Jiang, Y. Application of liquid desiccant system. In *Desiccant-Assisted Cooling: Fundamentals and Applications*; Nóbrega, C.E.L., Brum, N.C.L., Eds.; Springer: London, UK, 2014; pp. 249–281.
6. Li, Z.; Liu, X.; Jiang, Y.; Chen, X. New type of fresh air processor with liquid desiccant total heat recovery. *Energy Build.* **2005**, *37*, 587–593. [CrossRef]
7. Mumma, S.A. Designing dedicated outdoor air systems. *ASHRAE J.* **2001**, *43*, 28–32.
8. Liu, W.; Lian, Z.; Radermacher, R.; Yao, Y. Energy consumption analysis on a dedicated outdoor air system with rotary desiccant wheel. *Energy* **2007**, *32*, 1749–1760. [CrossRef]
9. Murphy, J. Smart dedicated outdoor air systems. *ASHRAE J.* **2006**, *48*, 30–37.
10. Dieckmann, J.; Roth, K.W.; Brodrick, J. Dedicated outdoor air systems. *ASHRAE J.* **2003**, *45*, 58–59.
11. Ruivo, C.R.; Hernández, F.F.; López, J.M.C. Influence of the desiccant wheel effectiveness method approaches, with fix and variable effectiveness parameters, on the performance results of an airport air-conditioning system. *Energy Convers. Manag.* **2015**, *94*, 458–471. [CrossRef]
12. Kim, M.H.; Park, J.Y.; Park, J.S.; Jeong, J.W. Application of desiccant systems for improving the performance of an evaporative cooling-assisted 100% outdoor air system in hot and humid climates. *J. Build. Perform. Simul.* **2015**, *8*, 173–190. [CrossRef]
13. Ge, G.; Xiao, F.; Xu, X. Model-based optimal control of a dedicated outdoor air-chilled ceiling system using liquid desiccant and membrane-based total heat recovery. *Appl. Energy* **2011**, *88*, 4180–4190. [CrossRef]
14. Niu, X.; Xiao, F.; Ge, G. Performance analysis of liquid desiccant based air-conditioning system under variable fresh air ratios. *Energy Build.* **2010**, *42*, 2457–2464. [CrossRef]
15. Jain, S.; Tripathi, S.; Das, R.S. Experimental performance of a liquid desiccant dehumidification system under tropical climates. *Energy Convers. Manag.* **2011**, *52*, 2461–2466. [CrossRef]
16. Katejanekarn, T.; Kumar, S. Performance of a solar-regenerated liquid desiccant ventilation pre-conditioning system. *Energy Build.* **2008**, *40*, 1252–1267. [CrossRef]
17. Humidification. Available online: http://www.daikinaircon.com/roomaircon/feature/kasitu (accessed on 20 March 2014).
18. Zhang, L.; Dang, C.; Hihara, E. Performance analysis of a no-frost hybrid air conditioning system with integrated liquid desiccant dehumidification. *Int. J. Refrig.* **2010**, *33*, 116–124. [CrossRef]
19. Kabeel, A.E. Dehumidification and humidification process of desiccant solution by air injection. *Energy* **2010**, *35*, 5192–5201. [CrossRef]
20. Liu, X.; Li, Z.; Jiang, Y.; Lin, B. Annual performance of liquid desiccant based independent humidity control HVAC system. *Appl. Therm. Eng.* **2006**, *26*, 1198–1207. [CrossRef]
21. De Antonellis, S.; Intini, M.; Joppolo, C.M.; Molinaroli, L.; Romano, F. Desiccant wheels for air humidification: An experimental and numerical analysis. *Energy Convers. Manag.* **2015**, *106*, 355–364. [CrossRef]
22. La, D.; Dai, Y.; Li, H.; Li, Y.; Kiplagat, J.K.; Wang, R. Experimental investigation and theoretical analysis of solar heating and humidification system with desiccant rotor. *Energy Build.* **2011**, *43*, 1113–1122. [CrossRef]
23. Wada, K.; Mashimo, K.; Takahashi, M.; Tanaka, K.; Toya, S.; Tateyama, R.; Miyamoto, K.; Yamaguchi, M. Desiccant humidity control system using waste heat of water source heat pump. *Trans. Jpn. Soc. Refrig. Air Cond. Eng.* **2011**, *26*, 501–510.
24. Fukudome, J. Desiccant Air Conditioner. U.S. Patent Application 13/583,354, 9 March 2011.
25. Mathiprakasam, B. Hybrid Vapor Compression and Desiccant Air Conditioning System. U.S. Patent No 4,430,864, 14 February 1984.
26. Purushothama, B. 3-Different Types of Humidification. In *Humidification and Ventilation Management in Textile Industry*; Elsevier Ltd.: San Diego, CA, USA, 2009; pp. 22–40.
27. Farley, R.D.; Franklin, D.H. Development of a humidifier for patient ventilation using a semi-permeable tube to minimize system condensate. *J. Biomed. Eng.* **1992**, *14*, 426–430. [CrossRef]
28. Vesley, D.; Anderson, J.; Halbert, M.M.; Wyman, L. Bacterial output from three respiratory therapy humidifying devices. *Respir. Care* **1979**, *24*, 228–234. [PubMed]
29. Thorn, A. Case study of a sick building: Could an integrated bio-psycho-social perspective prevent chronicity? In Proceedings of the Qualitative Evidence-Based Practice Conference, Coventry University, Coventry, UK, 15–17 May 2000.

30. Strindehag, O.; Josefsson, I.; Henningson, E. Emission of bacteria from air humidifiers. *Environ. Int.* **1991**, *17*, 235–241. [CrossRef]
31. Seppänen, O.; Fisk, W. Association of ventilation system type with SBS symptoms in office workers. *Indoor Air* **2002**, *12*, 98–112. [CrossRef] [PubMed]
32. Oie, S.; Masumoto, N.; Hironaga, K.; Koshiro, A.; Kamiya, A. Microbial contamination of ambient air by ultrasonic humidifier and preventive measures. *Microbios* **1991**, *72*, 161–166.
33. Xu, Z.; Xiao, Y.; Wang, Y. Experimental and theoretical studies on air humidification by a water spray at elevated pressure. *Appl. Therm. Eng.* **2007**, *27*, 2549–2558. [CrossRef]
34. Thörn, Å. The sick building syndrome: A diagnostic dilemma. *Soc. Sci. Med.* **1998**, *47*, 1307–1312.
35. Thörn, Å. Case study of a sick building. *Eur. J. Public Health* **2000**, *10*, 133–137.
36. Rozej, A.; Dudzinska, M.R.; Gaska-Jedruch, U. Seasonal variation and size distribution of bioaerosols in an air-conditioned auditorium—A case study. *Manag. Indoor Air Qual.* **2011**, *21*, 21–40.
37. Farnsworth, J.E.; Goyal, S.M.; Kim, S.; Kuehn, T.H.; Raynor, P.C.; Ramakrishnan, M.A.; Anantharaman, S.; Tang, W. Development of a method for bacteria and virus recovery from heating, ventilation, and air conditioning (HVAC) filters. *J. Environ. Monit.* **2006**, *8*, 1006–1013. [CrossRef] [PubMed]
38. Dahl, E. Physicochemical aspects of disinfection of water by means of ultrasound and ozone. *Water Res.* **1976**, *10*, 677–684. [CrossRef]
39. Kelly, D.; Kelly-Winterberg, K.; Sherman, D.; South, S. Rapid Sterilization of an Air Filter Medium. U.S. Patent Application 10/491,767, 2 February 2002.
40. Feldman, P.L.; Helfritch, D.J. Air Filter with Combined Enhanced Collection Efficiency and Surface Sterilization. U.S. Patent No. 6,245,132, 12 June 2001.
41. Green, C.F.; Scarpino, P.V. The use of ultraviolet germicidal irradiation (UVGI) in disinfection of airborne bacteria. *Environ. Eng. Policy* **2001**, *3*, 101–107. [CrossRef]
42. Noakes, C.J.; Fletcher, L.A.; Beggs, C.B.; Sleigh, P.A.; Kerr, K.G. Development of a numerical model to simulate the biological inactivation of airborne microorganisms in the presence of ultraviolet light. *J. Aerosol. Sci.* **2004**, *35*, 489–507. [CrossRef]
43. Ruivo, C.R.; Angrisani, G.; Minichiello, F. Influence of the rotation speed on the effectiveness parameters of a desiccant wheel: An assessment using experimental data and manufacturer software. *Renew. Energ.* **2015**, *76*, 484–493. [CrossRef]
44. Ruivo, C.R.; Costa, J.J.; Figueiredo, A.R.; Kodama, A. Effectiveness parameters for the prediction of the global performance of desiccant wheels—An assessment based on experimental data. *Renew. Energ.* **2012**, *38*, 181–187. [CrossRef]